

# Two-Point Boundary Value Problem Solutions to Spacecraft Formation Flying

Fanghua Jiang,\* Junfeng Li,† Hexi Baoyin,‡ and Yunfeng Gao§  
Tsinghua University, 100084 Beijing, People's Republic of China

DOI: 10.2514/1.43064

The two-point boundary value problem of a leader–follower spacecraft formation flying in unperturbed elliptical reference orbits is studied. The initial and final relative positions and times and the orbit of the leader are known, and the orbit of the follower must be determined. This problem will be called the relative Lambert's problem. First, we will show this relative Lambert's problem can be solved like the classical Lambert's problem. Then, a set of approximate analytic solutions are obtained through linearizing the Lagrange's time equation. Meanwhile, a simplified Newton–Raphson algorithm is applied to obtain numerical solutions, and the relevant quantities of the leader are used as initial conditions. Here, our special efforts are dedicated to the study of the periodic relative orbits of the follower. In particular, a set of first-order analytic solutions to the relative Lambert's problem are derived from the periodic solutions of Lawden's equations, and a constraint on the leader's true anomalies (implicitly in time) and relative positions is obtained. From that constraint on the radial/in-track plane of the leader local-vertical–local-horizontal frame, we found that, for specified initial and final times, the locus of final positions of the follower with fixed initial position is a straight line, and so is the locus of initial positions with fixed final position. Furthermore, for fixed initial and final positions, the transfer times with either specified initial time or final time can be expressed as the real roots of a cubic equation, for which there are at most three solutions. Several examples will be given to support these conclusions.

## Nomenclature

$a$	=	semimajor axis
$c$	=	chord
$c_j$	=	the $j$ th parameter with respect to orbit element differences
$E$	=	eccentric anomaly
$e, \mathbf{e}, \tilde{\mathbf{e}}$	=	eccentricity, eccentricity vector, and unit eccentricity vector
$f$	=	true anomaly
$i$	=	orbit inclination
$\mathbf{i}, \mathbf{j}, \mathbf{k}$	=	base vectors of the leader local-vertical–local-horizontal frame
$M$	=	mean anomaly
$n$	=	mean angular velocity
$p$	=	semilatus rectum
$R, \mathbf{R}$	=	radius and radius vector with respect to the Earth's center
$\mathbf{r}, r$	=	relative position vector and its magnitude
$s$	=	semiperimeter of triangle
$t$	=	time
$\mathbf{V}$	=	velocity vector with respect to the Earth
$\mathbf{v}$	=	relative velocity vector observed in the leader local-vertical–local-horizontal frame
$x, y, z$	=	follower relative position vector in the leader local-vertical–local-horizontal frame
$\alpha, \beta$	=	parameters of Lagrange's time equation
$\Delta$	=	difference between the follower and the leader
$\theta$	=	orbital transfer angle

$\mu$	=	gravity constant of the Earth
$\Omega$	=	right ascension of the ascending node
$\omega$	=	argument of perigee

## Subscripts

$f$	=	follower spacecraft
1, 2	=	relative to initial and final positions, respectively

## I. Introduction

COMPARED to single spacecraft, spacecraft formations offer greater flexibility and redundancy at a lower cost. So, much research on relative motion, formation design, and reconfiguration, spacecraft rendezvous, etc., has been conducted during the past decade. The relative motion of the moon with respect to the sun–Earth system was first studied by Hill [1]. Almost one century later, relative motion of spacecraft formation flying, that is, of one spacecraft (follower) following another (leader) in the leader local-vertical–local-horizontal (LVLH) frame, was studied by Clohessy and Wiltshire [2]. This was then extended from circular reference orbits to elliptical reference orbits independently by Lawden [3] and Tschauner and Hempel [4]. Since the 1990s, the literature on spacecraft formation flying has greatly expanded. Inalhan et al. [5] developed an initialization procedure for the solutions of the linearized relative motion equations for elliptical reference orbits. Schaub and Alfrend [6], and Gim and Alfrend [7] considered orbital perturbations such as the Earth's oblateness, which was absent in preceding studies. Carter [8], and Yamanaka and Ankersen [9] obtained a concise and simple state transition matrix, which is important to initial value problems involving the differential equations of relative motion. The two-point boundary value problem (TPBVP) of relative motion, here termed the relative Lambert's problem, where the initial and final relative positions, times, and the orbit of the leader are known, and the orbit of the follower is going to be determined, has not yet been sufficiently studied, though it plays a key role in formation configurations and orbit transfers of spacecraft formations. Deriving from the nonperiodic solution of the homogeneous Clohessy–Wiltshire equations, Mullins [10] obtained a set of solutions to TPBVP in circular reference orbits. In the framework of Keplerian motion, the TPBVP is also known as the classical

Received 8 January 2009; revision received 8 June 2009; accepted for publication 19 July 2009. Copyright © 2009 by the American Institute of Aeronautics and Astronautics, Inc. All rights reserved. Copies of this paper may be made for personal or internal use, on condition that the copier pay the \$10.00 per-copy fee to the Copyright Clearance Center, Inc., 222 Rosewood Drive, Danvers, MA 01923; include the code 0731-5090/09 and \$10.00 in correspondence with the CCC.

\*Ph.D. Candidate, School of Aerospace; jiangfh04@mails.thu.edu.cn.

†Professor, School of Aerospace; lijunf@tsinghua.edu.cn.

‡Associate Professor, School of Aerospace; baoyin@tsinghua.edu.cn (Corresponding Author).

§Associate Professor, School of Aerospace; gaoyunfeng@tsinghua.edu.cn.

Lambert's problem, to which the solution, namely, the orbit that passes through two fixed positions during specified transfer time, is determinable in terms of either the semimajor axis [11] or the transverse eccentricity component [12]. Shen and Tsotras [13] studied an optimal two-impulse rendezvous between two spacecraft in circular coplanar reference orbits with the application of multiple-revolution Lambert solutions. Guibout and Scheeres [14,15] applied generating functions connecting canonical transformations of Hamiltonian dynamics to solve the TPBVP of spacecraft formation as well as to study formation dynamics and design. In principle, their method is adequate for dealing with arbitrary gravity fields including the Earth's oblateness, but, in practice, the Taylor series expansion of the generating function seems rather complicated and laborious to solve. The purpose of this paper is to present some interesting and intuitive results for the TPBVP of spacecraft formation flying in unperturbed elliptical reference orbits by tractable methods, where existing results for the classical Lambert's problem and spacecraft formations are applied.

In a two-body problem, Lambert's theorem states [11] that "the orbital transfer time depends only upon the semimajor axis, the sum of the distances of the initial and final points of the arc from the center of force, and the length of the chord joining these points." The theorem can be stated mathematically, and the semimajor axis has to be found through iterative calculation. For relative motions of spacecraft formations, even after linearizing, the relative orbits are no longer conic sections but are generally on quadratic surfaces [16]. Therefore, the relative positions, transfer time, and the relative orbit will not have the same characteristic as that in Keplerian motion. Nevertheless, the follower's motion with respect to the Earth is still Keplerian. So, we first present that, without loss of generality, the relative Lambert's problem can be solved by the classical method. Suppose the relative distance between the follower and the leader is small compared to their geocentric distances, we can then linearize Lagrange's time equation of the classical Lambert's problem to obtain a first-order approximation. We will also show that numerical solutions can be obtained by the application of the simplified Newton-Raphson algorithm using the relevant quantities of the leader as the initial values, where the relative distance does not need to be small. In particular, we consider the periodic relative orbits, where not only the relative distances are small but also the relative state should satisfy the periodic condition. In addition to a set of first-order solutions to the relative Lambert's problem from the periodic solutions of Lawden's equations, we also obtain a constraint on the leader's true anomalies (implicitly in time) and relative positions. Furthermore, by analyzing the constraint, we find some interesting characteristic about the relative positions and the leader's true anomalies. They are quite different from results in the literature. But we should point out that these first-order solutions derived from the classical Lambert's problem are only applicable to the case of a very small relative distance between the follower and the leader, whereas the numerical solutions allow relatively large relative distance. More precisely, the results derived from the constraint on relative positions and times are only applicable to periodic relative orbits. The scope of this paper bears restating. It only considers the problem in the framework of Keplerian motion and spacecraft close formation is assumed. The excluded realistic perturbations, such as Earth oblateness, atmospheric drag, solar radiation pressure, etc., can be disruptive to formation design [17]. Therefore, active control is necessary to formation keeping. Nevertheless, as initial guess solutions, our analytic results can be very helpful for orbit transfers and orbit designs of spacecraft formation flying missions.

The rest of this paper is organized as follows: in the next section, we briefly introduce the classical Lambert's problem and its formulation, and state the relative Lambert's problem mathematically so as to be solved like the classical Lambert's problem. Then, in Sec. III, we will present the first-order approximate analytic solutions of the relative Lambert's problem through linearizing the classical problem, and present numerical solutions with the application of the simplified Newton-Raphson algorithm. Finally, in Sec. IV, as a particular and interesting case of periodic relative orbits, we discuss in detail the solutions of the relative Lambert's problem and the

constraint on relative positions and times. Examples are given to support the conclusions in each section. The Conclusions section ends this paper.

## II. Classical and Relative Lambert's Problems

The diagram of the relative Lambert's problem is depicted in Fig. 1. The leader moves on an elliptical orbit with the Earth as the focus. At the initial time  $t_1$ , the leader is on the point  $P_1$  and the follower is on  $P_{f1}$ . At the final time  $t_2$ , the leader is on the point  $P_2$  and the follower is on  $P_{f2}$ .  $\mathbf{R}_1$  and  $\mathbf{R}_2$  denote the position vectors of the leader relative to the Earth's center at  $t_1$  and  $t_2$ , respectively;  $\mathbf{r}_1$  and  $\mathbf{r}_2$  denote the position vectors of the follower relative to its leader at  $t_1$  and  $t_2$ , respectively. For the leader, the angle  $\theta$  between  $\mathbf{R}_1$  and  $\mathbf{R}_2$  is called the transfer angle of the leader, and the distance  $c$  between  $P_1$  and  $P_2$  is called the chord of the leader; for the follower, the counterparts are  $\theta_f$  and  $c_f$ . The relative motion of the follower with respect to the leader is usually observed in the leader LVLH frame, a noninertial frame attached to the leader. At the moment  $t_1$ , it is denoted by  $P_1xyz$ , with the  $x$  axis (radial direction) pointing radially away from the Earth's center,  $z$  axis (cross-track direction) coinciding with the direction of the leader's angular momentum vector, and  $y$  axis (in-track direction) completing the right-hand reference frame. Note that the two points  $P_{f1}$  and  $P_{f2}$  are described not in the inertial frame but in the leader LVLH frame. The goal is to find a follower orbit that passes through the points  $P_{f1}$  and  $P_{f2}$  at the times  $t_1$  and  $t_2$ , respectively. In this paper, we always assume that the orbit of the leader is given in terms of its six orbit elements, that is, semimajor axis  $a$ , eccentricity  $e$ , orbit inclination  $i$ , right ascension of the ascending node  $\Omega$ , argument of perigee  $\omega$ , and mean anomaly  $M_0$  (or true anomaly  $f_0$ ) at origin time  $t_0$ .

### A. Classical Lambert's Problem

The classical Lambert's problem can be stated as the "determination of an orbit, having a specified transfer time and connecting two position vectors" [11]. Especially, the determination of the orbit's semimajor axis is crucial. The geometry for the classical Lambert's problem can be illustrated in Fig. 1 by separately paying attention to the leader's Keplerian motion. The details about the classical Lambert's problem can be found in Battin's book [11], of which our concerns will be introduced briefly and necessarily.

The Lagrange's time equation for elliptical orbits to substantiate Lambert's theorem is

$$\sqrt{\mu}(t_2 - t_1) = a^{\frac{3}{2}}[(\alpha - \sin \alpha) - (\beta - \sin \beta)] \quad (1)$$

where  $\mu$  is the gravity constant, product of the Earth, and the universal gravitational constant. In addition, the Lagrange parameters  $\alpha$  and  $\beta$ , originally defined as  $\alpha = \varphi + \psi$  and  $\beta = \varphi - \psi$ , where  $\varphi$  and  $\psi$  are defined in terms of eccentricity and eccentric anomalies of the two points as  $\cos \varphi = e \cos[(E_2 + E_1)/2]$  and  $\psi = (E_2 - E_1)/2$ , have the relations in terms of  $R_1$ ,  $R_2$ , and  $c$  as

$$\begin{cases} R_1 + R_2 + c = 2a(1 - \cos \alpha) \\ R_1 + R_2 - c = 2a(1 - \cos \beta) \end{cases} \quad (2)$$

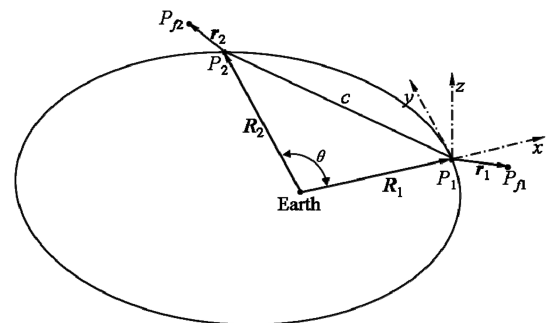


Fig. 1 Geometry of the relative Lambert's problem.

When the transfer angle is restricted to be greater than zero and less than 360 deg, and the eccentricity to be less than one (as we always do in this paper), it can be assumed that  $0 < \alpha < 2\pi$  and  $-\pi < \beta < \pi$ . In detail,  $\beta \geq 0$  for  $0 < \theta \leq \pi$ , and  $\beta < 0$  for  $\pi < \theta < 2\pi$ . In [18], it is pointed out that, if the flight time is greater than the flight time on the minimum-energy ellipse, then  $0 < \alpha \leq \pi$ ; otherwise,  $\pi < \alpha < 2\pi$ . Nevertheless, we will derive out a feasible discriminant in terms of eccentricity, initial true anomaly, and transfer angle. Since  $-\pi < \beta < \pi$ , the inequality  $\cos(\alpha/2) > 0$  is equivalent to  $2\cos(\alpha/2)\cos(\beta/2) = \cos\varphi + \cos\psi > 0$ , which is also equivalent to  $2\sin\psi(\cos\varphi + \cos\psi) > 0$  because  $0 < \psi < \pi$ . Substituting the definitions of  $\varphi$  and  $\psi$  into the preceding inequality, and applying the product to sum formula of trigonometric functions, we obtain

$$\sin(E_2 - E_1) + e(\sin E_2 - \sin E_1) > 0 \quad (3)$$

With the application of the relations between true anomaly and eccentric anomaly

$$\cos E = \frac{\cos f + e}{1 + e \cos f}, \quad \sin E = \frac{\sqrt{1 - e^2} \sin f}{1 + e \cos f} \quad (4)$$

and through simplification, it results in

$$(1 + e^2) \cos \frac{\theta}{2} + 2e \cos \left( f_1 + \frac{\theta}{2} \right) > 0 \quad (5)$$

where the relation  $\theta = f_2 - f_1$  is used. Finally, we obtain the inequality (5) equivalent to  $\cos(\alpha/2) > 0$ . To sum up for Eqs. (2), if  $0 < \theta \leq \pi$ , then  $\beta > 0$ , else  $\beta < 0$ ; if inequality (5) is satisfied, then  $0 < \alpha < \pi$ , else  $\pi \leq \alpha < 2\pi$ . Then the values of  $\alpha$  and  $\beta$  can be determined uniquely from  $R_1$ ,  $R_2$ ,  $c$ , and  $a$  in Eqs. (2). It is worth noting that the discriminant (5) is not available for the classical Lambert's problem because the eccentricity and true anomaly are unknown before obtaining the semimajor axis, but it will be useful in the relative Lambert's problem to evaluate the leader's Lagrange parameters  $\alpha$  and  $\beta$ .

The combination of Eqs. (1) and (2) can be used to solve for  $a$  through the iterative method if the initial and final positions are fixed, and the transfer time  $t_1 - t_2$  is specified, of which the details can be seen in [11]. However, the iterative method of the classical Lambert's problem is not our concern. Once the values of  $a$ ,  $\alpha$ , and  $\beta$  are known, the eccentricity can be obtained from the semilatus rectum expressed as [Eq. (6.110) in Ref. [11]]

$$p = a(1 - e^2) = \frac{R_1 R_2 (1 - \cos \theta) \sin \frac{1}{2}(\alpha + \beta)}{c \sin \frac{1}{2}(\alpha - \beta)} \quad (6)$$

where  $\alpha$  is always greater than  $\beta$  as long as the transfer angle is positive.

The normal vector of the orbit plane, that is, normalized angular momentum vector, denoted by  $\mathbf{k}$ , is determined through

$$\mathbf{k} = \frac{\mathbf{R}_1 \times \mathbf{R}_2}{\|\mathbf{R}_1 \times \mathbf{R}_2\|}, \quad 0 < \theta < \pi \quad (7)$$

Note that this is just valid for  $0 < \theta < \pi$ , and, for  $\pi < \theta < 2\pi$ ,  $\mathbf{k}$  should be its negative. In terms of orbit inclination  $i$  and right ascension of ascending node  $\Omega$ , the vector  $\mathbf{k}$  projected onto the Earth-centered inertial frame holds the form

$$\mathbf{k} = [\sin i \sin \Omega \quad -\sin i \cos \Omega \quad \cos i]^T \quad (8)$$

Therefore, we can obtain  $i$  and  $\Omega$  through the expressions

$$i = \cos^{-1} \mathbf{k}_z, \quad \Omega = \tan^{-1}(\mathbf{k}_x, -\mathbf{k}_y) \quad (9)$$

where  $\mathbf{k}_x$  ( $\mathbf{k}_y$  or  $\mathbf{k}_z$ ) denotes the component of the vector  $\mathbf{k}$  expressed by Eq. (7) along the  $x$  ( $y$  or  $z$ ) axis of the Earth-centered inertial frame, and  $\tan^{-1}(y, x)$  is the four-quadrant inverse tangent function, of which the singular case  $\tan^{-1}(0, 0)$  corresponding to  $\sin i = 0$  is assigned to be zero. The eccentricity vector  $\mathbf{e}$  holds the following form:

$$\sin^2 \theta \mathbf{e} = \left( \frac{p}{R_1} - 1 \right) \left( \frac{\mathbf{R}_1}{R_1} - \cos \theta \frac{\mathbf{R}_2}{R_2} \right) + \left( \frac{p}{R_2} - 1 \right) \left( \frac{\mathbf{R}_2}{R_2} - \cos \theta \frac{\mathbf{R}_1}{R_1} \right) \quad (10)$$

which is transformed from Eqs. (6.57) and (6.58) of [11]. However, using Eq. (10) to compute the eccentricity will lose significant digits when  $\sin \theta$  is near to zero. Therefore, we rebuild Eq. (10) and express the normalized eccentricity vector  $\mathbf{e}/e$ , denoted by  $\tilde{\mathbf{e}}$ , as

$$\tilde{\mathbf{e}} = \left[ \frac{1}{2e \cos(\theta/2)} \left( \frac{p}{R_1} + \frac{p}{R_2} - 2 \right) \right] \left[ \frac{1}{2 \cos(\theta/2)} \left( \frac{\mathbf{R}_1}{R_1} + \frac{\mathbf{R}_2}{R_2} \right) \right] + \left[ \frac{1}{2e \sin(\theta/2)} \left( \frac{p}{R_1} - \frac{p}{R_2} \right) \right] \left[ \frac{1}{2 \sin(\theta/2)} \left( \frac{\mathbf{R}_1}{R_1} - \frac{\mathbf{R}_2}{R_2} \right) \right] \quad (11)$$

which can also be expressed in terms of  $i$ ,  $\Omega$ , and  $\omega$  as

$$\tilde{\mathbf{e}} = \begin{bmatrix} \cos \omega \cos \Omega - \sin \omega \sin \Omega \cos i \\ \cos \omega \sin \Omega + \sin \omega \cos \Omega \cos i \\ \sin \omega \sin i \end{bmatrix} \quad (12)$$

Combining it with Eq. (10), the argument of perigee  $\omega$  can be worked out as

$$\omega = \tan^{-1}(\tilde{e}_z / \sin i, \cos \Omega \tilde{e}_x + \sin \Omega \tilde{e}_y) \quad (13)$$

where what  $\tilde{\mathbf{e}}_x$  ( $\tilde{\mathbf{e}}_y$  or  $\tilde{\mathbf{e}}_z$ ) denotes is analogous to  $\mathbf{k}_x$  ( $\mathbf{k}_y$  or  $\mathbf{k}_z$ ), and  $\sin i$  should be nonzero. If  $\sin i = 0$ , the argument of perigee should be evaluated by  $\tan^{-1}(\tilde{e}_y, \tilde{e}_x)$ . Two basic relations about Keplerian motion,  $p - R = eR \cos f$  and  $\mathbf{R} \cdot (\mathbf{k} \times \mathbf{e}) = eR \sin f$ , can be employed to obtain the true anomalies  $f_1$  and  $f_2$  at the initial position and final position, respectively:

$$f_l = \tan^{-1}[\mathbf{R}_l \cdot (\mathbf{k} \times \mathbf{e}), p - R_l], \quad l = 1, 2 \quad (14)$$

Based on the true anomaly  $f_l$  at the time  $t_l$ , it is easy to calculate the mean anomaly at any time, among which the relevant relations will be presented in following subsection.

Hereto, we have presented the process of determining the orbit by its six orbit elements starting from the initial and final position vectors, and the specified transfer time. Except for the semimajor axis and Lagrange parameters  $\alpha$  and  $\beta$ , which have to be solved by the numerical method, the other orbit elements possess analytic expressions. The transfer angle is restricted between 0 and 360 deg. And to determine the six orbit elements without singularity to the semimajor axis and eccentricity, the transfer angle is not allowed to be 180 deg. The velocity vectors with respect to the center of force at the initial and final points are

$$\begin{cases} \mathbf{V}_1 = \frac{\sqrt{\mu p}}{R_1 R_2 \sin \theta} [(\mathbf{R}_2 - \mathbf{R}_1) + \frac{R_2}{p} (1 - \cos \theta) \mathbf{R}_1] \\ \mathbf{V}_2 = \frac{\sqrt{\mu p}}{R_1 R_2 \sin \theta} [(\mathbf{R}_2 - \mathbf{R}_1) - \frac{R_1}{p} (1 - \cos \theta) \mathbf{R}_2] \end{cases} \quad (15)$$

where the transfer angle is not allowed to be 180 deg because two collinear vectors can not uniquely determine the orbit plane.

## B. Relative Lambert's Problem

In this subsection, we will show that, if the leader's orbit elements are given, the follower's orbit connecting two fixed relative position vectors at a specified time can also be determined, like that in the classical Lambert's problem.

The leader's true anomaly at the time  $t_l$  (hereafter, subscript  $l$  with 1 and 2 denotes initial and final positions, respectively) can be obtained by first calculating the mean anomaly through

$$M_l = M_0 + n(t_l - t_0) \quad (16)$$

then solving Kepler's equation

$$M_l = E_l - e \sin E_l \quad (17)$$

for the eccentric anomaly, and finally substituting it into

$$\tan \frac{f_l}{2} = \sqrt{\frac{1+e}{1-e}} \tan \frac{E_l}{2} \quad (18)$$

To solve Kepler's equation, we apply the iteration algorithm as well as the initial value selection presented in [19]. The radius and radius vector of the leader at the initial and final times have the forms

$$\mathbf{R}_l = R_l(\cos f_l \tilde{\mathbf{e}} + \sin f_l \mathbf{q}), \quad R_l = \frac{a(1-e^2)}{1+e \cos f_l} \quad (19)$$

where the normalized eccentricity vector  $\tilde{\mathbf{e}}$  holds the form Eq. (12), and  $\mathbf{q} = \mathbf{k} \times \tilde{\mathbf{e}}$ , of which the vector  $\mathbf{k}$  holds the form Eq. (8).

Because  $P_{f1}$  and  $P_{f2}$  are both fixed in the leader LVLH frame, we can assume the relative position vectors  $\mathbf{r}_l$  and  $\mathbf{r}_2$  with the form

$$\mathbf{r}_l = x_l \mathbf{i}_l + y_l \mathbf{j}_l + z_l \mathbf{k} \quad (20)$$

where  $\mathbf{i}_l, \mathbf{j}_l, \mathbf{k}$  are the base vectors of the leader LVLH frame at the time  $t_l$  ( $l = 1, 2$ ), holding the forms

$$\begin{aligned} \mathbf{i}_l &= \mathbf{R}_l / R_l = \cos f_l \tilde{\mathbf{e}} + \sin f_l \mathbf{q} \\ \mathbf{j}_l &= \mathbf{k} \times \mathbf{i}_l = -\sin f_l \tilde{\mathbf{e}} + \cos f_l \mathbf{q} \end{aligned} \quad (21)$$

and  $x_l, y_l, z_l$  are the given relevant coordinate components. Because the leader's orbit is Keplerian, the base vector  $\mathbf{k}$  is invariant with respect to time.

Up to this time, the position vectors of the follower relative to the Earth's center corresponding to the initial and final times can be expressed through

$$\mathbf{R}_{f1} = \mathbf{R}_l + \mathbf{r}_l \quad (22)$$

Therefore, the follower's orbit can be determined through the same process as in the classical Lambert's problem introduced in preceding subsection. It is worth noting that the transfer angle of the follower  $\theta_f$  has two admissible selections. One is  $\cos^{-1}[(\mathbf{R}_{f2} \cdot \mathbf{R}_{f1}) / (R_{f2} R_{f1})]$  and another is  $2\pi - \cos^{-1}[(\mathbf{R}_{f2} \cdot \mathbf{R}_{f1}) / (R_{f2} R_{f1})]$ . Here, we select it according to the range of the leader's transfer angle

$$\theta_f = \begin{cases} \cos^{-1} \frac{\mathbf{R}_{f1} \cdot \mathbf{R}_{f2}}{R_{f1} R_{f2}}, & 0 < \theta \leq \pi \\ 2\pi - \cos^{-1} \frac{\mathbf{R}_{f1} \cdot \mathbf{R}_{f2}}{R_{f1} R_{f2}}, & \pi < \theta < 2\pi \end{cases} \quad (23)$$

To sum up, for the relative Lambert's problem, of which the leader's orbit is given, and the initial and final relative position vectors are given with the form Eq. (20), the semimajor axis  $a_f$  of the follower's orbit connecting the initial and final relative position vectors at the times  $t_1$  and  $t_2$ , respectively, can be determined through solving the following Lagrange's time equations:

$$\begin{cases} \sqrt{\mu}(t_2 - t_1) = a_f^3 [\alpha_f - \sin \alpha_f - (\beta_f - \sin \beta_f)] \\ R_{f1} + R_{f2} + c_f = 2a_f(1 - \cos \alpha_f) \\ R_{f1} + R_{f2} - c_f = 2a_f(1 - \cos \beta_f) \end{cases} \quad (24)$$

where  $R_{f1}$  and  $R_{f2}$  are, respectively, the magnitudes of  $\mathbf{R}_{f1}$  and  $\mathbf{R}_{f2}$  evaluated through Eq. (22). The chord is calculated through

$$c_f = \|\mathbf{R}_{f2} - \mathbf{R}_{f1}\| = \sqrt{R_{f1}^2 + R_{f2}^2 - 2R_{f1}R_{f2}\cos\theta_f} \quad (25)$$

The follower's transfer angle  $\theta_f$  is evaluated through Eq. (23). Once the follower's semimajor axis is obtained, the other five orbit elements as well as the velocity vectors of the follower with respect to the Earth can be calculated through Eqs. (6–15). Then the quantities of the follower, such as  $a_f, \alpha_f, \beta_f, \mathbf{R}_{f1}, \mathbf{R}_{f2}, c_f$ , and  $\theta_f$ , should be used in place of that of the leader, such as  $a, \alpha, \beta, \mathbf{R}_l, \mathbf{R}_2, c$ , and  $\theta$ , respectively, provided that  $\mathbf{R}_{f1}$  and  $\mathbf{R}_{f2}$  are not collinear vectors, namely, the following continued equality is not satisfied:

$$\frac{z_2}{z_1} = \frac{R_2 + x_2}{(R_1 + x_1)\cos\theta + y_1\sin\theta} = \frac{y_2}{-(R_1 + x_1)\sin\theta + y_1\cos\theta} \quad (26)$$

The relative velocity of the follower with respect to the leader LVLH frame, denoted by  $\mathbf{v}_l$ , is related with the velocities of the leader  $\mathbf{V}_l$  and the follower  $\mathbf{V}_{f1}$  with respect to the Earth through  $\mathbf{v}_l = \mathbf{V}_{f1} - \mathbf{V}_l - \boldsymbol{\omega}_l \times \mathbf{r}_l$ , where  $\boldsymbol{\omega}_l$  is the angular velocity vector of the leader with the form

$$\boldsymbol{\omega}_l = \dot{f}_l \mathbf{k} = \sqrt{\frac{\mu}{p^3}}(1 + e \cos f_l)^2 \mathbf{k} \quad (27)$$

### III. First-Order Analytic Solutions and Numerical Solutions

In the preceding section, we have presented that the relative Lambert's problem can be solved like the classical Lambert's problem by existing numerical iteration. In spacecraft formation flying, generally, the distance between the follower and the leader is small compared to their geocentric distances, so that the relative Lambert's problem could be approximated to be a somewhat simple one if accurate solutions are not necessary. Therefore, we will derive first-order analytic solutions and show that the simplified Newton–Raphson iteration with the leader's semimajor axis and Lagrange parameters as its initial conditions can result in solutions of high accuracy.

#### A. First-Order Analytic Solutions

We have obtained that the follower's semimajor axis  $a_f$  and the Lagrange parameters  $\alpha_f$  and  $\beta_f$  satisfy Eqs. (24). With the application of  $\Delta \mathbf{R}_1 = \mathbf{r}_1$  and  $\Delta \mathbf{R}_2 = \mathbf{r}_2$ , where  $\Delta$  denotes the difference between the follower and the leader, we can expand  $\Delta \mathbf{R}_l = \|\mathbf{R}_l + \mathbf{r}_l\| - R_l$  as

$$\begin{aligned} \Delta R_l &= R_l \left[ 1 + 2 \frac{x_l r_l}{r_l R_l} + \left( \frac{r_l}{R_l} \right)^2 \right]^{\frac{1}{2}} - R_l = x_l + \frac{y_l^2 + z_l^2}{2R_l} \\ &\quad + \frac{x_l(x_l^2 - r_l^2)}{2R_l^2} + \dots \end{aligned} \quad (28)$$

where  $R_l$  has the form Eq. (19), and expand  $\Delta c = \|\mathbf{R}_2 + \mathbf{r}_2\| - R_2$  as

$$\Delta c = c \left[ 1 + \frac{2A + B}{c^2} \right]^{\frac{1}{2}} - c = \frac{A}{c} + \frac{B}{2c} - \frac{A^2}{2c^3} - \frac{AB}{2c^3} + \frac{A^3}{2c^5} + \dots \quad (29)$$

where  $A = (\mathbf{R}_2 - \mathbf{R}_1) \cdot (\mathbf{r}_2 - \mathbf{r}_1)$  and  $B = \|\mathbf{r}_2 - \mathbf{r}_1\|^2$ . Note that the preceding expansions for  $\Delta R_l$  and  $\Delta c$  are both truncated to the third order. It can be seen that  $A/c^2$  is first-order small and  $B/c^2$  is second-order small. By applying Eqs. (21), their expressions yield the forms

$$A = R_2(x_2 - x_1 \cos \theta - y_1 \sin \theta) - R_1(x_2 \cos \theta - y_2 \sin \theta - x_1) \quad (30)$$

$$\begin{aligned} B &= (x_2 \cos \theta - y_2 \sin \theta - x_1)^2 + (x_2 \sin \theta + y_2 \cos \theta - y_1)^2 \\ &\quad + (z_2 - z_1)^2 \end{aligned} \quad (31)$$

The cosine of the follower's transfer angle

$$\cos \theta_f = \frac{(\mathbf{R}_2 + \mathbf{r}_2) \cdot (\mathbf{R}_1 + \mathbf{r}_1)}{\|\mathbf{R}_2 + \mathbf{r}_2\| \|\mathbf{R}_1 + \mathbf{r}_1\|} \quad (32)$$

can be expanded around that of the leader,  $\cos \theta = \mathbf{R}_2 \cdot \mathbf{R}_1 / (R_2 R_1)$ , as

$$\begin{aligned} \cos \theta_f &= \left( \frac{\mathbf{R}_1 \cdot \mathbf{R}_2 + \mathbf{R}_1 \cdot \mathbf{r}_2 + \mathbf{r}_1 \cdot \mathbf{R}_2 + \mathbf{r}_1 \cdot \mathbf{r}_2}{R_1 R_2} \right) \\ &\times \left( 1 + 2 \frac{x_1}{r_1} \frac{r_1}{R_1} + \frac{r_1^2}{R_1^2} \right)^{-\frac{1}{2}} \left( 1 + 2 \frac{x_2}{r_2} \frac{r_2}{R_2} + \frac{r_2^2}{R_2^2} \right)^{-\frac{1}{2}} \\ &= \left[ \cos \theta + \frac{x_2 \cos \theta - y_2 \sin \theta}{R_2} + \frac{x_1 \cos \theta + y_1 \sin \theta}{R_1} \right. \\ &\quad \left. + \frac{(x_1 x_2 + y_1 y_2) \cos \theta + (x_2 y_1 - x_1 y_2) \sin \theta + z_1 z_2}{R_1 R_2} \right] \\ &\times \left[ \sum_{n=0}^{\infty} P_n \left( -\frac{x_1}{r_1} \right) \left( \frac{r_1}{R_1} \right)^n \right] \left[ \sum_{n=0}^{\infty} P_n \left( -\frac{x_2}{r_2} \right) \left( \frac{r_2}{R_2} \right)^n \right] \quad (33) \end{aligned}$$

where the Legendre polynomial [20]

$$(1 - 2xt + t^2)^{-1/2} = \sum_{n=0}^{\infty} P_n(x)(t)^n, \quad |x| \leq 1, |t| < 1 \quad (34)$$

is used. Truncating series (33) to the second order yields

$$\begin{aligned} \cos \theta_f &\approx \cos \theta - \left( \frac{y_2}{R_2} - \frac{y_1}{R_1} \right) \sin \theta - \frac{(y_1^2 + z_1^2) \cos \theta + 2x_1 y_1 \sin \theta}{2R_1^2} \\ &\quad - \frac{(y_2^2 + z_2^2) \cos \theta + 2x_2 y_2 \sin \theta}{2R_2^2} + \frac{z_1 z_2 + y_1 y_2 \cos \theta}{R_1 R_2} \quad (35) \end{aligned}$$

Expanding Eqs. (24) with respect to  $\Delta a$ ,  $\Delta \alpha$ , and  $\Delta \beta$  to reserve the first-order term results in a set of linear equations:

$$\begin{aligned} &\begin{bmatrix} \frac{3}{2}n(t_2 - t_1) & 1 - \cos \alpha & -(1 - \cos \beta) \\ 1 - \cos \alpha & \sin \alpha & 0 \\ 1 - \cos \beta & 0 & \sin \beta \end{bmatrix} \begin{bmatrix} \frac{\Delta a}{a} \\ \Delta \alpha \\ \Delta \beta \end{bmatrix} \\ &= \begin{bmatrix} 0 \\ \frac{1}{2a} \Delta(R_1 + R_2 + c) \\ \frac{1}{2a} \Delta(R_1 + R_2 - c) \end{bmatrix} \quad (36) \end{aligned}$$

Now it is easy to obtain the solutions for  $\Delta a$ ,  $\Delta \alpha$ , and  $\Delta \beta$ :

$$\Delta a = -\frac{1}{F} \left[ \sin \frac{\alpha - \beta}{2} \Delta(R_1 + R_2) + \sin \frac{\alpha + \beta}{2} \Delta c \right] \quad (37)$$

$$\begin{aligned} \Delta \alpha &= \frac{1}{4aF \sin(\alpha/2)} \left\{ \left[ 3n(t_2 - t_1) \cos \frac{\beta}{2} \right. \right. \\ &\quad \left. \left. + 2 \sin \frac{\beta}{2} (\cos \alpha - \cos \beta) \right] \Delta(R_1 + R_2) \right. \\ &\quad \left. + \left[ 3n(t_2 - t_1) \cos \frac{\beta}{2} + 2 \sin \frac{\beta}{2} (2 - \cos \alpha - \cos \beta) \right] \Delta c \right\} \quad (38) \end{aligned}$$

$$\begin{aligned} \Delta \beta &= \frac{1}{4aF \sin(\beta/2)} \left\{ \left[ 3n(t_2 - t_1) \cos \frac{\alpha}{2} \right. \right. \\ &\quad \left. \left. + 2 \sin \frac{\alpha}{2} (\cos \alpha - \cos \beta) \right] \Delta(R_1 + R_2) \right. \\ &\quad \left. - \left[ 3n(t_2 - t_1) \cos \frac{\alpha}{2} - 2 \sin \frac{\alpha}{2} (2 - \cos \alpha - \cos \beta) \right] \Delta c \right\} \quad (39) \end{aligned}$$

where

$$F = 3n(t_2 - t_1) \cos \frac{\alpha}{2} \cos \frac{\beta}{2} - 4 \sin^3 \frac{\alpha}{2} \cos \frac{\beta}{2} + 4 \sin^3 \frac{\beta}{2} \cos \frac{\alpha}{2} \quad (40)$$

Based on Eqs. (28) and (29),  $\Delta(R_1 + R_2)$  and  $\Delta c$  can be approximated to the first order or higher order. Here, we just truncate them to the first order:

$$\Delta R_1 \approx x_1, \quad \Delta R_2 \approx x_2 \quad (41)$$

$$\Delta c \approx \frac{R_1(x_1 - x_2 \cos \theta + y_2 \sin \theta) + R_2(x_2 - x_1 \cos \theta - y_1 \sin \theta)}{c} \quad (42)$$

Note that we just consider the case  $0 < \theta < 2\pi$ , so that  $0 < \alpha < 2\pi$ ,  $-\pi < \beta < \pi$ ,  $\alpha > \beta$ , and  $\sin(\alpha/2) \neq 0$ . Moreover,  $F$  is also always nonzero, which can be proved as follows. Substitute Eq. (1) for  $n(t_2 - t_1)$  into Eq. (40) and reform it as

$$F = \cos \frac{\alpha}{2} \cos \frac{\beta}{2} [Q(\beta) - Q(\alpha)] \quad (43)$$

where

$$Q(x) = 4 \sin^2 \frac{x}{2} \tan \frac{x}{2} - 3(x - \sin x) \quad (44)$$

When  $\alpha = \pi$ , the possibility for  $F = 0$  is  $\cos(\beta/2) = 0$ , whereas it is impossible because  $-\pi < \beta < \pi$ . So we can exclude the isolated point  $\alpha = \pi$  from  $Q(\alpha)$ . It is easy to get the derivative of  $Q(x)$  with respect to  $x$  with the form  $Q'(x) = 2 \sin^2(x/2) \tan^2(x/2)$ , which is never less than zero. Therefore,  $Q(x)$  is a monotonic increasing function in its fields of definitions, such as  $(-\pi, \pi)$ ,  $(\pi, 3\pi)$ , etc., and the possible case for different  $\alpha$  and  $\beta$  with equivalent value of  $Q(x)$  is that  $-\pi < \beta < 0$  and  $\pi < \alpha < 2\pi$ . Then, it can be derived from Eqs. (2) that  $\sin(\alpha/2) = \sqrt{s/(2a)}$ ,  $\cos(\alpha/2) = -\sqrt{1 - s/(2a)}$ ,  $\sin(\beta/2) = -\sqrt{(s - c)/(2a)}$ , and  $\cos(\beta/2) = \sqrt{1 - (s - c)/(2a)}$ , where  $s = (R_1 + R_2 + c)/2$ . Substituting these relations into Eq. (40) yields

$$\begin{aligned} F &= -\frac{1}{a^2} [s^{3/2} \sqrt{2a - s + c} - (s - c)^{3/2} \sqrt{2a - s}] \\ &\quad - \frac{3n(t_2 - t_1)}{2a} \sqrt{2a - s} \sqrt{2a - s + c} \quad (45) \end{aligned}$$

Since  $2a \geq s \geq c$  and  $n(t_2 - t_1) > 0$ , it is obvious that  $F < 0$ . And so, it can be concluded that  $F$  is always nonzero for  $0 < \theta < 2\pi$ . The singularity that  $\beta = 0$  in Eq. (39) can be removed. In fact, when  $\beta = 0$ , the third equation of Eqs. (36) will become equivalent to  $0 = \Delta(R_1 + R_2 - c)$ . This equation is self-evident if  $\Delta R_1$ ,  $\Delta R_2$ , and  $\Delta c$  expressed by Eqs. (28) and (29) are uniformly truncated to the first order, otherwise it is self-contradictory. For this exception, we can originally expand the third equation of Eqs. (24) to the second order:  $a(\Delta \beta)^2 = \Delta(R_1 + R_2 - c)$ . Then, choose the positive value

$$\Delta \beta = \left[ \frac{(y_2 + y_1)^2 + (z_2 - z_1)^2}{2a(R_1 + R_2)} + \frac{y_1^2 + z_1^2}{2aR_1} + \frac{y_2^2 + z_2^2}{2aR_2} \right]^{\frac{1}{2}} \quad (46)$$

Thus, as first-order approximation, Eqs. (36) will not be singular for the case  $\beta \neq 0$ . For the case  $\beta = 0$ , we use Eq. (46) instead of Eq. (39) to evaluate  $\Delta \beta$ .

Once we obtain the first-order approximations of  $\Delta a$ ,  $\Delta \alpha$ ,  $\Delta \beta$ ,  $\Delta R_1$ ,  $\Delta R_2$ , and  $\Delta c$  and truncate the difference of the transfer angle to the first order from Eq. (35)

$$\Delta \theta \approx \frac{y_2}{R_2} - \frac{y_1}{R_1} \quad (47)$$

we can calculate the other five orbit elements of the follower as well as the velocity vectors with respect to the center of force through Eqs. (6–15).

## B. Numerical Solutions

The Newton–Raphson algorithm, of which the  $m$ th iteration holds the form  $\mathbf{u}^{m+1} = \mathbf{u}^m - \mathbf{F}'(\mathbf{u}^m)^{-1} \mathbf{F}(\mathbf{u}^m)$ , is widely used to solve systems of  $k$  (nonlinear) equations,  $\mathbf{F}(\mathbf{u}) = 0$ , where  $\mathbf{F}: \mathbf{R}^k \rightarrow \mathbf{R}^k$  is continuously differentiable and  $\mathbf{u}$  is a  $k$ -dimensions column vector. Replacing  $\mathbf{F}'(\mathbf{u}^m)$  by  $\mathbf{F}'(\mathbf{u}^0)$  is beneficial to reducing computational load, and then it is called a simplified Newton–Raphson algorithm. Denote  $\mathbf{u} = [a_f/a, \alpha_f, \beta_f]^T$  and apply this simplified algorithm

to solve the relative Lambert's problem expressed by Eqs. (24). Especially, we choose the leader's semimajor axis  $a$ , parameters  $\alpha$  and  $\beta$  as the initial values, namely,  $\mathbf{u}^0 = [1.0, \alpha, \beta]^T$ . The inverse of the  $3 \times 3$  Jacobian matrix  $\mathbf{F}'(\mathbf{u}^0)$  and the column vector  $\mathbf{F}(\mathbf{u}^m)$  have the following analytic expressions:

$$\mathbf{F}'(\mathbf{u}^0)^{-1} = \frac{1}{8F \sin^2 \frac{\alpha}{2} \sin^2 \frac{\beta}{2}} \times \begin{bmatrix} 4s\alpha s\beta & -2(1-\alpha)s\beta & 2s\alpha(1-c\beta) \\ -4(1-\alpha)s\beta & 3nt_{12}s\beta + 2(1-c\beta)^2 & -2(1-\alpha)(1-c\beta) \\ -4s\alpha(1-c\beta) & 2(1-\alpha)(1-c\beta) & 3nt_{12}s\alpha - 2(1-\alpha)^2 \end{bmatrix} \quad (48)$$

$$\mathbf{F}(\mathbf{u}^m) = \begin{bmatrix} (u_1^m)^{3/2}(u_2^m - su_2^m - u_3^m + su_3^m) - nt_{12} \\ 2u_1^m(1 - cu_2^m) - \frac{1}{a}(R_{f1} + R_{f2} + c_f) \\ 2u_1^m(1 - cu_3^m) - \frac{1}{a}(R_{f1} + R_{f2} - c_f) \end{bmatrix} \quad (49)$$

where  $F$  is expressed by Eq. (40),  $t_{12}$  denotes  $t_2 - t_1$ , and the compact notations  $sx = \sin(x)$  and  $cx = \cos(x)$  are applied for  $\alpha$ ,  $\beta$ ,  $u_3^m$ , and  $u_2^m$ . A tolerance and a maximum number of iterations are needed to continue the iterations until either the maximum one of the three variables' absolute differences between the  $(m+1)$ th and  $m$ th iterations is less than the tolerance, or the maximum number of iterations is exceeded. As indicated in preceding subsection, the possibility for  $8F \sin(\alpha/2) \sin(\beta/2) = 0$ , namely, the Jacobian matrix is singular so as to have no inverse, is only when  $\beta = 0$ , which troubles the iteration not at all as long as we evaluate  $\beta$  by Eq. (46).

Having obtained the numerical solutions of  $a_f$ ,  $\alpha_f$ , and  $\beta_f$ , we then compute  $R_{f1}$ ,  $R_{f2}$ ,  $c_f$ , and  $\theta_f$  without truncation, and finally substitute them into Eqs. (6–15) to compute the other five orbit elements of the leader as well as the velocity vectors with respect to the center of force.

### C. Examples

Set the leader's six orbit elements as

$$[a, e, i, \Omega, \omega, f_1] \\ = [1.0, 0.1, 1.0 \text{ rad}, 0.0 \text{ rad}, 0.0 \text{ rad}, 0.0 \text{ rad}]$$

Here, both the leader's semimajor axis  $a$  and the gravity constant  $\mu$  are normalized to one, so the unit of time is  $T/2\pi$ , where  $T$  is leader's orbit period. Given the initial relative position vector  $\mathbf{r}_1$  with coordinate components in the leader LVLH frame  $(x_1, y_1, z_1) = (1.0, 1.0, 1.0) \times 10^{-3}$ , and the final relative position vector  $\mathbf{r}_2$  with  $(x_2, y_2, z_2) = (0.0, 0.0, 0.0)$ , we can evaluate the order of magnitude of the relative motion, that is, the relative distance divided by the leader's geocentric distance, that of  $10^{-3}$ . Let the transfer time increase from  $\pi/4$  ( $T/8$ ) to  $3\pi/4$  ( $3T/8$ ) by step  $\pi/1000$ . Then, we can calculate the relevant follower's orbit elements through the first-order approximation and numerical iteration, respectively. Consequently, the follower's actual initial and final relative positions in the leader LVLH frame can also be computed through relative position equations [Eqs. (1) in [16]], generally used to study spacecraft formation flying. The distance between the actual relative position and the expected one, termed position error, can be used to evaluate the feasibility of the two methods.

The position error curves are depicted in Fig. 2. Here, the tolerance for numerical iteration is set to  $10^{-14}$ . The numbers of actual iterations for all the transfer times considered are uniformly five. Figure 2 shows that the initial and final position errors caused by first-order approximations are both of the magnitude  $10^{-6}$ , second-order small, as expected. Whereas those caused by numerical iterations are rather small, owing to the tolerance is set to be very small so that the results are almost accurate. This could substantiate the feasibility of both the first-order approximation and the numerical iteration. If the relative distance between the follower and the leader is too large, such as  $(x_1, y_1, z_1) = (0.0, 0.0, 0.0)$  and  $(x_2, y_2, z_2) = (0.1, 0.1, 0.1)$ , and other parameters remain the same as before, the first-order

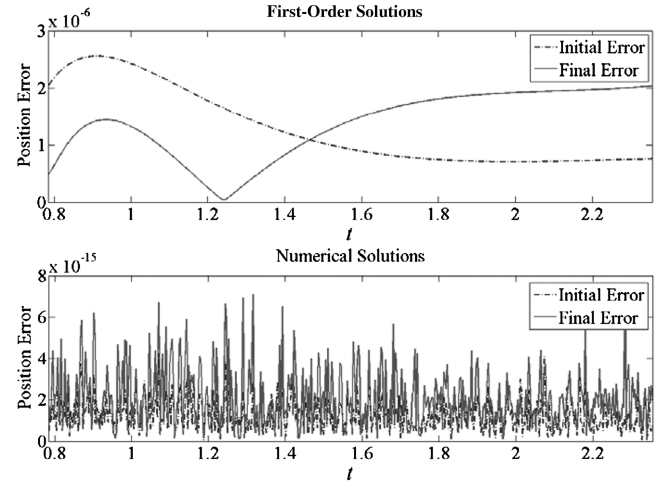


Fig. 2 Position errors of first-order solutions and numerical solutions.

approximation will cause large errors, as shown in Fig. 3, whereas the numerical iteration still results in solutions of high accuracy. The difference from the former case is that the number of actual iterations does not remain five, but decreases from 125 to 18 when the transfer time increases from  $\pi/4$  to  $3\pi/4$ . Although additional tests show that the numerical iteration will not converge if the relative distance increases further, such as  $(x_2, y_2, z_2) = (0.5, 0.5, 0.5)$ , the numerical iteration and first-order approximation still shed light on the study of the two-point boundary value problem of spacecraft formation flying, where the relative distance is always small.

## IV. First-Order Solutions Satisfying Periodic Condition

In close formations, to eliminate the secular term, the semimajor axes of the follower and the leader should be equivalent. In other words, the periodic condition of Lawden's equations [5] should be satisfied. It has been proved [21] that this periodic condition is equivalent to the first-order term of the semimajor axis difference between the follower and the leader being zero. Therefore, the first-order analytic solution of semimajor axis difference expressed by Eq. (37) in the preceding section will be set to zero in the following consideration.

### A. First-Order Solutions Satisfying Periodic Condition

Substitute Eqs. (41) and (42) into Eq. (37) and let  $\Delta a = 0$ . We obtain the constraint on relative positions

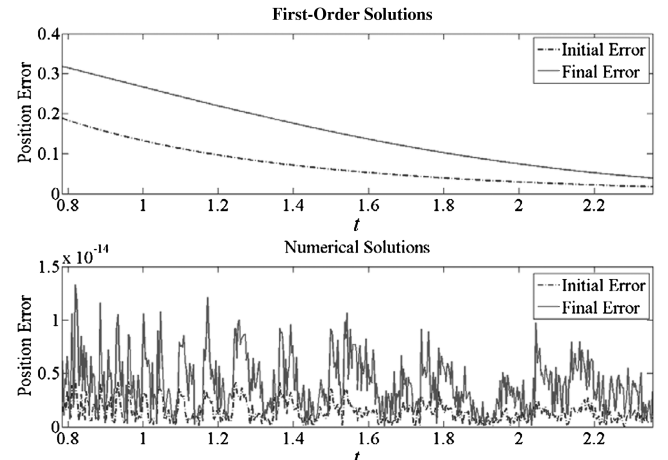


Fig. 3 Position errors of first-order solutions and numerical solutions for large distances.

$$[1 + e \cos(f_1 + \theta)](x_1 - x_2 \cos \theta + y_2 \sin \theta) + (1 + e \cos f_1)(x_2 - x_1 \cos \theta - y_1 \sin \theta) + (1 - \cos \theta)(x_1 + x_2) = 0 \quad (50)$$

which is, of course, just first-order approximate. Among the derivation, the relations Eqs. (6) and (19) are used. This constraint directly indicates that, to achieve a follower orbit with the semimajor axis first-order approximate to that of the leader, the leader's initial true anomaly  $f_1$ , eccentricity  $e$ , transfer angle  $\theta$ , and the relative positions projected onto the  $x/y$  plane of the leader's LVLH frame are not independent, but should satisfy a relationship.

Although derived from the variation of Lagrange's time equation for the Lambert problem of elliptic orbits, this constraint can also be obtained through the relative position equations in terms of either orbit element differences or initial relative state. As presented in [16], the relative position equations have the parameterized forms

$$\begin{cases} x = -c_1 \cos f + c_2 e \sin f \\ y = c_2(1 + e \cos f) + c_1 \sin f(1 + \frac{1}{1+e \cos f}) + \frac{(1-e)c_3}{1+e \cos f} \\ z = \frac{1}{1+e \cos f}[c_4 \sin f + (1-e)c_5 \cos f] \end{cases} \quad (51)$$

where the five parameters  $\{c_1, c_2, c_3, c_4, c_5\}$  are associated either with the leader's orbit elements and orbit element differences between the follower and the leader, or with initial ( $f = 0$ ) relative position  $(x_0, y_0, z_0)$  and initial relative velocity  $(x'_0, y'_0, z'_0)$ , written together as

$$\begin{cases} c_1 = a\Delta e = -\frac{1+e}{e}(2x_0 + y'_0) \\ c_2 = \frac{a\Delta M}{\sqrt{1-e^2}} = \frac{x'_0}{e} \\ c_3 = a(1+e)(\Delta\omega + \Delta\Omega \cos i) = \frac{1+e}{e(1-e)}[-(1+e)x'_0 + ey_0] \\ c_4 = a(1-e^2)(\Delta i \cos \omega + \Delta\Omega \sin \omega \sin i) = (1+e)z'_0 \\ c_5 = a(1+e)(\Delta i \sin \omega - \Delta\Omega \cos \omega \sin i) = \frac{1+e}{1-e}z_0 \end{cases} \quad (52)$$

where  $(\cdot)'$  denotes the derivative of  $(\cdot)$  with respect to  $f$ , observed in the leader LVLH frame. Note that the mean anomaly difference between two orbits is not constant unless their semimajor axes are exactly equal. But as long as the periodic condition is satisfied, the semimajor axis difference between the two orbits is second-order small, so that the mean anomaly difference varies very slowly with respect to time. An alternative treatment is to regard  $\Delta M$  in Eqs. (52) as the instantaneous value of the moment  $f = 0$ . As a first-order approximation, the true anomaly difference  $\Delta f$  can be evaluated in terms of  $\Delta M$  and  $\Delta e$  through [Eq. (A13) of [21]]:

$$\Delta f = \frac{1}{1-e^2}(2 + e \cos f) \sin f \Delta e + \frac{(1+e \cos f)^2}{(1-e^2)^{3/2}} \Delta M \quad (53)$$

To obtain the derivative with respect to time, multiplying  $(\cdot)'$  by  $df/dt$  expressed by Eq. (27) is needed. Consequently, the relative velocity equations of the periodic solutions to Lawden's equations can also be parameterized as

$$\begin{cases} x' = c_1 \sin f + c_2 e \cos f \\ y' = -c_2 e \sin f + c_1[\cos f + \frac{\cos f + e}{(1+e \cos f)^2}] + \frac{e(1-e)c_3 \sin f}{(1+e \cos f)^2} \\ z' = \frac{1}{(1+e \cos f)^2}[c_4(\cos f + e) - (1-e)c_5 \sin f] \end{cases} \quad (54)$$

Because the follower orbit should pass through the two relative positions  $\mathbf{r}_1$  and  $\mathbf{r}_2$  at the leader's true anomalies  $f_1$  and  $f_2$ , respectively, we can replace  $f$  by  $f_1$  and  $f_2$ , and  $(x, y, z)$  by  $(x_1, y_1, z_1)$  and  $(x_2, y_2, z_2)$  in Eqs. (51), respectively, to obtain a set of six equations with five unknowns. Generally, because the number of equations is more than that of unknowns by one, these equations are not independent but should satisfy a constraint condition. It is not difficult to solve the two equations arising from the first equation of Eqs. (51) at  $f_1$  and  $f_2$ , respectively, for  $c_1$  and  $c_2$  as

$$\begin{cases} c_1 = \frac{x_2 \sin f_1 - x_1 \sin f_2}{\sin \theta} \\ c_2 = \frac{x_2 \cos f_1 - x_1 \cos f_2}{e \sin \theta} \end{cases} \quad (55)$$

And for  $c_4$  and  $c_5$ ,

$$\begin{cases} c_4 = \frac{z_2(1+e \cos f_2) \cos f_1 - z_1(1+e \cos f_1) \cos f_2}{\sin \theta} \\ c_5 = \frac{z_1(1+e \cos f_1) \sin f_2 - z_2(1+e \cos f_2) \sin f_1}{(1-e) \sin \theta} \end{cases} \quad (56)$$

where  $\theta = f_2 - f_1$ . Then, substituting Eqs. (55) into the two equations arising from the second equation of Eqs. (51) at  $f_1$  and  $f_2$ , respectively, besides the solution of  $c_3$  with the form

$$c_3 = \frac{1}{1-e} \left[ y_1(1+e \cos f_1) - c_2 + (2+e \cos f_1) \frac{x_1 \cos \theta - x_2}{\sin \theta} \right] \quad (57)$$

we can also obtain a constraint condition, which is exactly the same as Eq. (50). After getting the five parameters expressed in terms of the leader's orbit elements including the initial and final true anomalies, and, importantly, the relative position coordinates of the initial and final positions, we can obtain the orbit element differences of the follower with respect to the leader by inversely solving Eqs. (52) as follows:

$$\begin{cases} \Delta e = c_1/a \\ \Delta M = c_2 \sqrt{1-e^2}/a \\ \Delta i = [c_4 \cos \omega + c_5(1-e) \sin \omega]/[a(1-e^2)] \\ \Delta \Omega = [c_4 \sin \omega - c_5(1-e) \cos \omega]/[a(1-e^2) \sin i] \\ \Delta \omega = c_3/[a(1+e)] - [c_4 \sin \omega - c_5(1-e) \cos \omega]/[a(1-e^2) \tan i] \end{cases} \quad (58)$$

If necessary, the initial relative state can be similarly solved. Because the difference of the semimajor axis is second-order small, we set  $\Delta a = 0$  as an approximation. Substituting the five parameters expressed by Eqs. (55–57) into the relative velocity expressions Eqs. (54), and evaluating them at  $f_1$  and  $f_2$ , respectively, we can obtain the relative velocities at the initial and final positions.

In Eqs. (55–57), the leader's transfer angle of 180 deg causes the follower's orbit elements to be singular. The reason is that the orbit plane cannot be determined, as indicated in the previous section. That is to say, the orbit inclination and right ascension of the ascending node are both arbitrary. Nevertheless, the leader's transfer angle of 180 deg does not mean the follower's transfer angle is also exactly 180 deg. It is readily seen from Eq. (35) that, when the leader's transfer angle  $\theta$  is 180 deg, no matter what the coordinates of the two relative position vectors are, the follower's transfer angle  $\theta_f$  is also 180 deg in first-order approximation. Therefore, it is not surprising that the first-order relative position equations cannot be used to solve for the relative Lambert's problem with the leader's transfer angle of 180 deg. Second-order ones may be feasible for this case, provided that neither  $y_2/R_2 - y_1/R_1$  nor  $z_2/R_2 + z_1/R_1$  are equal to zero, which can be derived from Eq. (35) by substituting  $\theta = 180$  deg into it and setting  $\theta_f = 180$  deg.

## B. Relative Positions Satisfying Periodic Condition

We have shown that the relative Lambert's problem can be transformed into the classical Lambert's problem, and, furthermore, when the relative distance is small, it can be linearized to be solved analytically. So generally, once the initial and final times are specified, and given the leader's orbit elements, for any pair of initial and final relative positions, the follower's orbit can be determined. However, for close formation, to satisfy the periodic condition, these quantities are not arbitrary, but should satisfy the constraint (50). In this subsection, we will analyze this constraint in detail to disclose some interesting characteristics. Now that the leader's transfer angle is not allowed to be 0 or 360 deg, we could divide Eq. (50) by  $\sin(\theta/2)$  and reform it as

$$\left(2 \sin \frac{\theta}{2} - e \sin f_1 \cos \frac{\theta}{2}\right)x_1 - \cos \frac{\theta}{2}(1 + e \cos f_1)y_1 + \left[2 \sin \frac{\theta}{2} + e \sin(f_1 + \theta) \cos \frac{\theta}{2}\right]x_2 + \cos \frac{\theta}{2}[1 + e \cos(f_1 + \theta)]y_2 = 0 \quad (59)$$

### 1. Loci of Relative Positions with Equal Transfer Time

Assume that the initial time  $t_1$ , final time  $t_2$ , the leader's orbit elements (mainly  $a$ ,  $e$ ,  $M_0$ ), and the initial relative position with coordinates  $(x_1, y_1, z_1)$  are given or specified. Employing Eqs. (16–18), the leader's initial and final true anomalies  $f_1$  and  $f_2$ , as well as the transfer angle  $\theta$  can be calculated. It is obvious that regarding  $e$ ,  $f_1$ ,  $\theta$ ,  $x_1$ , and  $y_1$  as known, the set of final relative positions expressed by Eq. (59) form a straight line on the leader's radial/in-track coordinate plane. Spatially, it is plane perpendicular to this coordinate plane. Because the  $z$ -axis component is absent in the constraint, hereafter we always restrict our discussion in the leader's radial/in-track coordinate plane. Particularly, for circular orbits, the straight line equation is simply

$$y_2 - y_1 = -2 \tan \frac{\theta}{2}(x_2 + x_1) \quad (60)$$

Similarly, fixing the final relative position with coordinates  $(x_2, y_2, z_2)$ , the set of initial relative positions form another straight line on the leader's radial/in-track coordinate plane. For circular reference orbits, the straight line equation is Eq. (60), too, regarding  $x_2$  and  $y_2$  as known. In addition, if a pair of initial and final relative positions,  $(x_1, y_1)$  and  $(x_2, y_2)$ , satisfy constraint (59), it is obvious that any pair of initial and final relative positions with coordinates, respectively,  $(\lambda x_1, \lambda y_1)$  and  $(\lambda x_2, \lambda y_2)$ , where  $\lambda$  is a nonzero real number, satisfy the same constraint.

Let us take the following example:  $e = 0.5$ ,  $f_1 = \pi/3$ ,  $\theta = 2\pi/3$ ,  $(x_1, y_1) = (4.0, 2.0)$ , and  $(x_2, y_2) = (-3.5, 5.0)$ , where the two position coordinates, nondimensionalized appropriately, are chosen intentionally to satisfy the constraint. As depicted in Fig. 4, the point 1, 2, and  $O$  denote  $(x_1, y_1)$ ,  $(x_2, y_2)$ , and the origin, respectively. The transfer time from point 1 to 2, here denoted by  $t_{12}$  for convenience, is equal to the time spent by the leader traveling from  $f_1$  to  $f_1 + \theta$ . The locus of final positions, to which the transfer time spent by the follower orbits traveling from the fixed initial point 1 is  $t_{12}$ , is the solid line passing through point 2. Analogously, the locus of initial positions, from which the transfer time spent by the follower orbits traveling to the fixed final point 2 is  $t_{12}$ , is the solid line passing through point 1. Each line parallel to the line connecting point 1 and 2 intersects the line passing through the origin  $O$  and point 1 at one

point, and intersects the line passing through the origin  $O$  and point 2 at another point. The time spent by the follower orbit traveling from the former point to the latter point is  $t_{12}$ , too. The dash-dot lines in Fig. 4 illustrate this situation. It is worth noting that all the conclusions are based on the first-order approximation, which requires the relative distance between the follower and the leader to always be a small quantity, compared to their geocentric distances. The farther the relative position departs from the origin, the larger the error of the approximate results.

### 2. Solutions for the Transfer Time from Relative Positions

Assume that the initial time  $t_1$ , the leader's orbit elements (mainly  $a$ ,  $e$ ,  $M_0$ ), and the initial and final relative positions with coordinates  $(x_1, y_1, z_1)$  and  $(x_2, y_2, z_2)$  are given or specified. Then, constraint (59) becomes an equation with the transfer angle as unknown, which seems somewhat complicated to solve. Anyway, once the transfer angle is obtained, we can transform it into the transfer time through inversely employing Eqs. (16–18). To solve Eq. (59) for  $\theta$ , first apply the sum formulas of trigonometric functions to  $\sin(f_1 + \theta)$  and  $\cos(f_1 + \theta)$ , then divide the consequent equation by  $\cos(\theta/2)$  and denote  $\tan(\theta/2)$  by  $w$ , and, finally, employ the relations  $\cos \theta = (1 - w^2)/(1 + w^2)$  and  $\sin \theta = 2w/(1 + w^2)$ . Multiplying the consequent equation by  $1 + w^2$ , we can at last transform Eq. (59) into

$$g_3 w^3 + g_2 w^2 + g_1 w + g_0 = 0 \quad (61)$$

where

$$g_3 = 2(x_1 + x_2) \quad (62)$$

$$g_2 = -ex_1 \sin f_1 - (1 + e \cos f_1)y_1 - ex_2 \sin f_1 + (1 - e \cos f_1)y_2 \quad (63)$$

$$g_1 = 2x_1 + 2(1 + e \cos f_1)x_2 - 2e \sin f_1 y_2 \quad (64)$$

$$g_0 = -ex_1 \sin f_1 - (1 + e \cos f_1)y_1 + ex_2 \sin f_1 + (1 + e \cos f_1)y_2 \quad (65)$$

This is a cubic equation, for which the solutions hold analytic forms [22]:

$$\begin{cases} w_1 = -\frac{1}{3} \frac{g_2}{g_3} + (\sqrt[3]{S + \sqrt{D}} + \sqrt[3]{S - \sqrt{D}}) \\ w_2 = -\frac{1}{3} \frac{g_2}{g_3} - \frac{1}{2} (\sqrt[3]{S + \sqrt{D}} + \sqrt[3]{S - \sqrt{D}}) + \frac{\sqrt{3}}{2} j (\sqrt[3]{S + \sqrt{D}} - \sqrt[3]{S - \sqrt{D}}) \\ w_3 = -\frac{1}{3} \frac{g_2}{g_3} - \frac{1}{2} (\sqrt[3]{S + \sqrt{D}} + \sqrt[3]{S - \sqrt{D}}) - \frac{\sqrt{3}}{2} j (\sqrt[3]{S + \sqrt{D}} - \sqrt[3]{S - \sqrt{D}}) \end{cases} \quad (66)$$

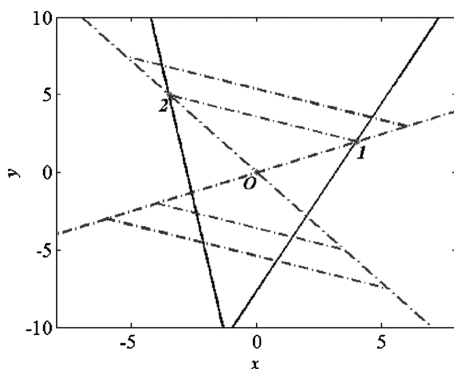


Fig. 4 Loci of relative positions with equal transfer time.

where  $j$  is the imaginary unit, and the expressions of  $S$  and  $D$  are

$$S = \frac{9g_1g_2g_3 - 27g_0g_3^2 - 2g_2^3}{54g_3^3} \quad (67)$$

$$D = S^2 + \left(\frac{3g_1g_3 - g_2^2}{9g_3^2}\right)^3 = \frac{1}{108g_3^4} (4g_0g_2^3 + 4g_1^3g_3 + 27g_0^2g_3^2 - 18g_0g_1g_2g_3 - g_2^2g_2^2) \quad (68)$$

provided  $g_3$ , that is,  $x_1 + x_2$ , is nonzero. If  $D$  is positive, then there is one real root for the problem considered (the other two are complex roots, which are excluded); if  $D$  is negative, then there are three real roots; if  $D = 0$ , then there is one real root (a triple root, corresponding



to the case  $g_2^2 = 3g_1g_3$ ) or two real roots (a single and a double root, corresponding to the case  $g_2^2 > 3g_1g_3$ ). If  $w > 0$ , the leader's transfer angle  $\theta = 2\tan^{-1}(w)$ , else  $\theta = 2\pi - 2\tan^{-1}(-w)$ .

If  $x_1 + x_2 = 0$ , besides the trivial solution  $w = \infty$ , corresponding to  $\theta = \pi$ , the other solutions can be obtained by solving  $g_2w^2 + g_1w + g_0 = 0$ , of which the discriminant  $g_1^2 - 4g_2g_0$  determines the number of real roots, as well known.

It is known that, for a cubic equation, there is at least one real root. However, the zero root, corresponding to  $\theta = 0$  or  $2\pi$ , is out of our consideration. The necessary and sufficient condition for Eq. (61) to have zero root is  $g_0 = 0$ . Furthermore, if  $g_2^2 - 4g_1g_3 < 0$ , zero root is the only real root. Therefore, the combination conditions comprising  $g_0 = 0$  and  $g_2^2 - 4g_1g_3 < 0$  correspond to the problem considered of no solution. Analogously, if the final time is specified and the initial time is free, we can regard  $f_2$  as known and write  $f_1$  as  $f_2 - \theta$  to solve for  $\theta$  in Eq. (59). Thus, another cubic equation can be obtained. The conclusions about solution existence are similar to the case of specifying the initial time.

Through the preceding analyses, we can conclude that, once the initial and final relative positions are fixed, the initial time is specified, and the leader's orbit elements are given, the follower's orbits, which connect the two relative positions and satisfy the periodic condition, can be determined in first-order approximation. The number of possible orbits is from null to three, and the relevant discriminants are analytically expressible. Note that the periodic condition means essentially that the semimajor axis of the follower is equal to that of the leader in first-order approximation. Specifying the final time rather than the initial time leads to analogous conclusions.

### C. Examples

#### 1. Loci of Relative Positions with Fixed Initial or Final Position

Set the orbit elements of the leader as

$$[a, e, i, \Omega, \omega, f_1] \\ = [1.0, 0.2, 1.0 \text{ rad}, 1.0 \text{ rad}, 1.0 \text{ rad}, 0.0 \text{ rad}]$$

and  $f_2 = 2\pi/3$ . Given the initial point  $(x_1, y_1)$  with coordinates  $(\sqrt{3.0}, 2.0) \times 10^{-3}$ , from Eq. (59), the final points  $(x_2, y_2)$  should satisfy the equation of line  $y_2 = -7.0x_2/\sqrt{3.0} - 4.0 \times 10^{-3}$ . Select eight points with  $x_2 = 1.0 \times 10^{-3}$ ,  $0.5 \times 10^{-3}$ ,  $0.0 \times 10^{-3}$ ,  $-0.5 \times 10^{-3}$ ,  $-1.0 \times 10^{-3}$ ,  $-1.5 \times 10^{-3}$ ,  $-2.0 \times 10^{-3}$ , and  $-2.5 \times 10^{-3}$ , respectively. The order of magnitude of the relative motion is  $10^{-3}$ . Because the combination of any final point with a fixed initial point satisfies the constraint of the periodic condition, we can calculate the relevant follower's orbit elements through two methods. One is the first-order approximation method, as presented in Sec. IV.A; another is numerical iteration, as presented in Sec. III.B. Their orbits are depicted in Fig. 5. The dotted straight line denotes the locus of the final points, which intersects the orbits at the final points. The dash-dot lines denote the follower orbits obtained through

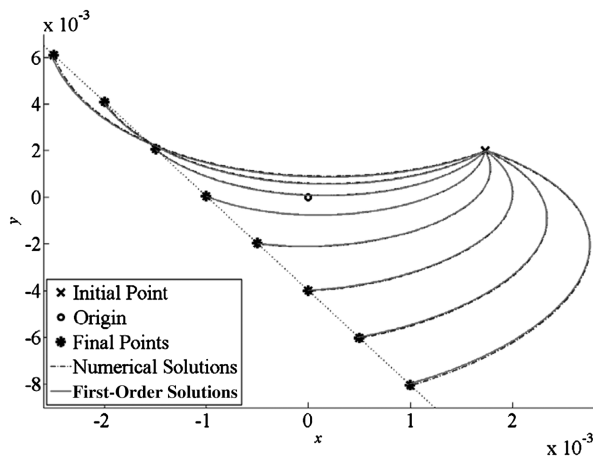


Fig. 5 Locus of final points with fixed initial point.

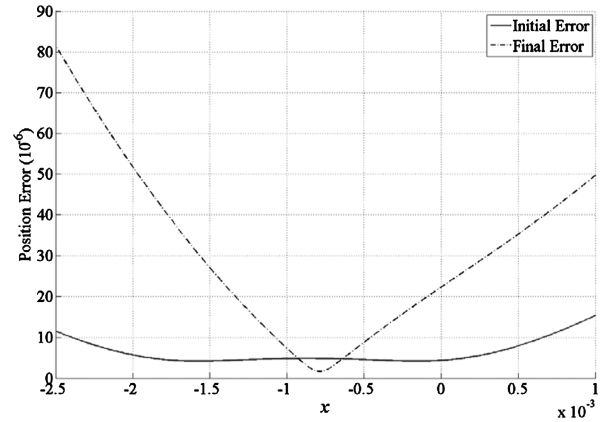


Fig. 6 Relative position errors of first-order approximations.

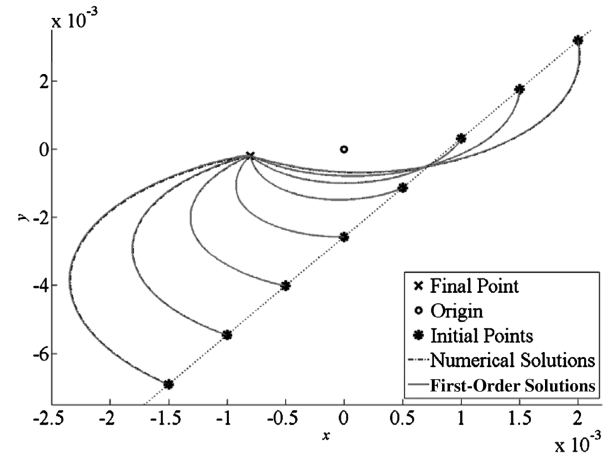


Fig. 7 Locus of initial points with fixed final point.

numerical iterations, whereas the solid lines correspond to first-order approximations. Let  $x_2$  increase from  $-2.5 \times 10^{-3}$  to  $1.0 \times 10^{-3}$  by step  $1.0 \times 10^{-5}$ , and then, through the method of first-order approximation, we can obtain the relation curves of the follower's position errors with respect to  $x_2$ , as shown in Fig. 6. The initial error is always of the magnitude  $10^{-6}$ , second-order small, as expected, but the final error is not so, except around  $x_2$  with the value of about  $-0.75 \times 10^{-3}$ , according to the assertion that the farther the relative position departs from the origin, the larger the error of the approximate results.

Analogously, fix the final point  $(x_2, y_2)$  with coordinates  $(-0.8, -0.2) \times 10^{-3}$ . Select eight points with  $x_1 = -1.5 \times 10^{-3}$ ,  $-1.0 \times 10^{-3}$ ,  $-0.5 \times 10^{-3}$ ,  $0.0 \times 10^{-3}$ ,  $0.5 \times 10^{-3}$ ,  $1.0 \times 10^{-3}$ ,  $1.5 \times 10^{-3}$ , and  $2.0 \times 10^{-3}$ , respectively. The follower's orbits are depicted in Fig. 7. During the time that the true anomaly of the leader

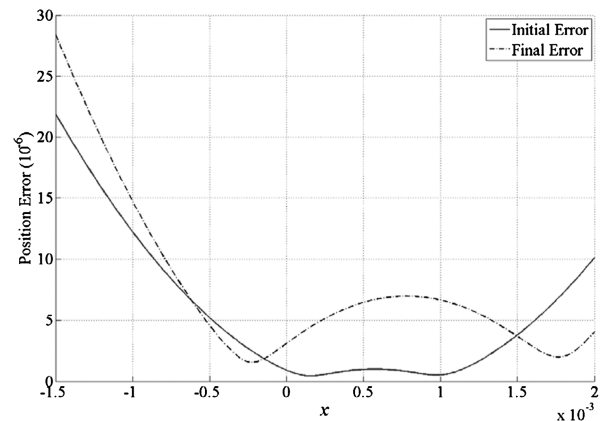


Fig. 8 Relative position errors of first-order approximations.

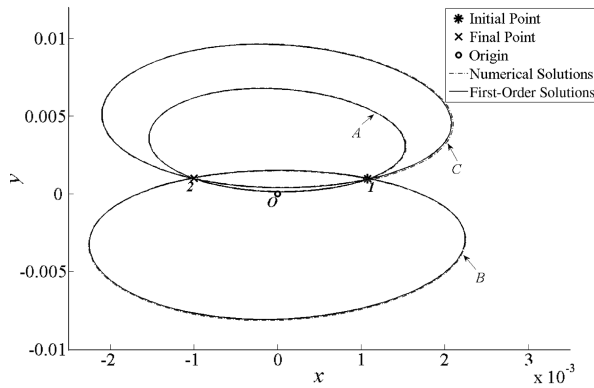


Fig. 9 Three periodic orbits pass through fixed initial and final positions during different times.

increases from  $f_1$  to  $f_2$ , the follower's orbits are expected to travel from different initial points to the fixed final points, respectively. The position error curves are depicted in Fig. 8. Differing from the former case, both the initial error and final error is of the magnitude  $10^{-6}$  only in almost the same range near to the origin.

## 2. Solutions for the Transfer Time from Relative Positions

Set the orbit elements of the leader as

$$[a, e, i, \Omega, \omega, f_1] \\ = [1.0, 0.1, 1.0 \text{ rad}, 0.0 \text{ rad}, 0.0 \text{ rad}, 0.0 \text{ rad}]$$

For  $x_1 = 1.08 \times 10^{-3}$ ,  $y_1 = 0.96 \times 10^{-3}$ ,  $x_2 = -1.00 \times 10^{-3}$ , and  $y_2 = 1.00 \times 10^{-3}$ , it can be determined that, in Eq. (61), there are three real roots for  $w$ , namely, 0.9231,  $-0.5205$ , and  $0.5724$ . The three transfer angles are 1.4909, 5.3234, and 1.0397 rad, corresponding to the orbits A, B, and C, respectively, shown in Fig. 9. It can be calculated that the transfer times for orbits A, B, and C are 0.2058T, 0.8722T, and 0.1391T, respectively, where T is the leader's orbit period. That is to say, for the given initial position  $(x_1, y_1)$ , marked by 1, and final position  $(x_2, y_2)$ , marked by 2, there are three follower orbits satisfying the period condition. During their respective transfer times, orbits A and C travel the short arc, but orbit B travels the long arc. The initial position error for orbit A is  $6.78 \times 10^{-6}$ , for B  $2.32 \times 10^{-5}$ , and for C  $1.90 \times 10^{-5}$ ; the final position error for orbit A is  $3.87 \times 10^{-5}$ , for B  $6.30 \times 10^{-5}$ , and for C  $5.92 \times 10^{-5}$ , approximately second-order small as expected.

## V. Conclusions

The two-point boundary value problem, or relative Lambert's problem, of a leader-follower spacecraft formation flying in unperturbed elliptical reference orbits is studied. Given the initial and final relative positions, times, and the orbit elements of the leader, the relative Lambert's problem can be cast into the same form as the classical one so that the follower's orbit can be determined by solving for the semimajor axis just as in the classical Lambert's problem. Because the relative distance between the follower and the leader is small compared to their geocentric distances, and if we limit the leader's transfer angle between 0 and 360 deg, Lagrange's time equations (including two parameter equations) of the classical Lambert's problem can be linearized and solved for the semimajor axis of the follower analytically to get the follower's orbit. Also, numerical solutions employing the simplified Newton-Raphson algorithm are obtained by using the relevant quantities of the leader as initial values. Several examples show that the approximate solutions are accurate enough when the relative positions are close to the origin, and that the errors of the numerical solutions are still very small even when the relative positions are some distance from their origins.

In this paper, the periodic relative orbits are studied in detail. When the semimajor axis of the orbits between the leader and follower are approximated to the first order, the other five orbit element

differences between the follower and the leader can be obtained in terms of the relative position coordinates and the leader's initial and final true anomalies. Furthermore, we obtained a constraint on the leader's true anomalies (implicitly in time) and relative positions based on the linearized Lagrange's time equation and the periodic solutions of Lawden's equations. From the constraint on the radial/in-track plane of the leader local-vertical-local-horizontal frame, we found 1) for a specified time period, the locus of final positions of the follower with fixed initial position is a straight line, and so is the locus of initial positions with fixed final position; and 2) for fixed initial and final positions, with either initial time or final time specified, the transfer times can be expressed as the real roots of a cubic equation, for which there are at most three solutions. Because these conclusions are derived under linearization, they are only valid for close spacecraft formations. That is, as can be seen in the examples, the farther the follower departs from the leader, the larger the error of the approximate results.

## Acknowledgment

This work was supported by the National Natural Science Foundation of China (No. 10832004 and No. 10602027).

## References

- [1] Hill, G. W., "Researches in the Lunar Theory," *American Journal of Mathematics*, Vol. 1, No. 1, 1878, pp. 5–26. doi:10.2307/2369430
- [2] Clohessy, W., and Wiltshire, R., "Terminal Guidance System for Satellite Rendezvous," *Journal of the Aero/Space Sciences*, Vol. 27, No. 9, 1960, pp. 653–678.
- [3] Lawden, D. F., *Optimal Trajectories for Space Navigation*, Butterworths, London, 1963, pp. 79–86.
- [4] Tschauner, J., and Hempel, P., "Rendezvous with a Target in an Elliptical Orbit," *Astronautica Acta*, Vol. 11, No. 2, 1965, pp. 104–109.
- [5] Inalhan, G., Tillerson, M., and How, J. P., "Relative Dynamics and Control of Spacecraft Formations in Eccentric Orbits," *Journal of Guidance, Control, and Dynamics*, Vol. 25, No. 1, 2002, pp. 48–59. doi:10.2514/2.4874
- [6] Schaub, H., and Alfriend, K. T., " $J_2$  Invariant Relative Orbits for Spacecraft Formations," *Celestial Mechanics and Dynamical Astronomy*, Vol. 79, No. 2, 2001, pp. 77–95. doi:10.1023/A:1011161811472
- [7] Gim, D. W., and Alfriend, K. T., "State Transition Matrix of Relative Motion for the Perturbed Noncircular Reference Orbit," *Journal of Guidance, Control, and Dynamics*, Vol. 26, No. 6, 2003, pp. 956–971. doi:10.2514/2.6924
- [8] Carter, T. E., "State Transition Matrices for Terminal Rendezvous Studies: Brief Survey and New Example," *Journal of Guidance, Control, and Dynamics*, Vol. 21, No. 1, 1998, pp. 148–155. doi:10.2514/2.4211
- [9] Yamanaka, K., and Ankersen, F., "New State Transition Matrix for Relative Motion on an Arbitrary Elliptical Orbit," *Journal of Guidance, Control, and Dynamics*, Vol. 25, No. 1, 2002, pp. 60–66. doi:10.2514/2.4875
- [10] Mullins, L. D., "Initial Value and Two Point Boundary Value Solutions to the Clohessy-Wiltshire Equations," *The Journal of the Astronautical Sciences*, Vol. 40, No. 4, 1992, pp. 487–501.
- [11] Battin, R. H., *An Introduction to the Mathematics and Methods of Astrodynamics, Revised Edition*, AIAA Education Series, AIAA, Reston, VA, 1999, Chaps. 6–7.
- [12] Avanzini, G., "A Simple Lambert Algorithm," *Journal of Guidance, Control, and Dynamics*, Vol. 31, No. 6, 2008, pp. 1587–1594. doi:10.2514/1.36426
- [13] Shen, H., and Tsiotras, P., "Optimal Two-Impulse Rendezvous Using Multiple-Revolution Lambert Solutions," *Journal of Guidance, Control, and Dynamics*, Vol. 26, No. 1, 2003, pp. 50–61. doi:10.2514/2.5014
- [14] Guibout, V. M., and Scheeres, D. J., "Solving Relative Two-Point Boundary Value Problems: Spacecraft Formation Flight Transfers Application," *Journal of Guidance, Control, and Dynamics*, Vol. 27, No. 4, 2004, pp. 693–704. doi:10.2514/1.11164
- [15] Guibout, V. M., and Scheeres, D. J., "Spacecraft Formation Dynamics and Design," *Journal of Guidance, Control, and Dynamics*, Vol. 29, No. 1, 2006, pp. 121–133.

- doi:10.2514/1.13002
- [16] Jiang, F., Li, J., Baoyin, H., and Gao, Y., "Study on Relative Orbit Geometry of Spacecraft Formations in Elliptical Reference Orbits," *Journal of Guidance, Control, and Dynamics*, Vol. 31, No. 1, 2008, pp. 123–134.  
doi:10.2514/1.30394
- [17] Sabol, C., Burns, R., and McLaughlin, C. A., "Satellite Formation Flying Design and Evolution," *Journal of Spacecraft and Rockets*, Vol. 38, No. 2, 2001, pp. 270–278.  
doi:10.2514/2.3681
- [18] Prussing, J. E., "Geometrical Interpretation of the Angles  $\alpha$  and  $\beta$  in Lambert's Problem," *Journal of Guidance and Control*, Vol. 2, No. 5, 1979, pp. 442–443.
- doi:10.2514/3.55905
- [19] Murray, C. D., and Dermott, S. F., *Solar System Dynamics*, Cambridge Univ. Press, Cambridge, England, U.K., 1999, pp. 35–36.
- [20] Andrews, L. C., *Special Functions for Engineers and Applied Mathematicians*, Macmillan, New York, 1985, Chap. 4.
- [21] Jiang, F. H., Li, J. F., and Baoyin, H., "Approximate Analysis for Relative Motion of Satellite Formation Flying in Elliptical Orbits," *Celestial Mechanics and Dynamical Astronomy*, Vol. 98, No. 1, 2007, pp. 31–66.  
doi:10.1007/s10569-007-9067-8
- [22] Abramowitz, M., and Stegun, I. A., *Handbook of Mathematical Functions with Formulas, Graphs, and Mathematical Tables*, Ninth Printing, Dover, New York, 1972, p. 17.